

## Supporting Information

belonging to

### Structure of $\beta$ -Lactoglobulin Microgels Formed during Heating as Revealed by Small-Angle X-Ray Scattering and Light Scattering

*Christian Moitzi<sup>+</sup>, Laurence Donato<sup>‡</sup>, Christophe Schmitt<sup>‡</sup>, Lionel Bovetto<sup>‡</sup>, Graeme Gillies<sup>+</sup>, and Anna Stradner<sup>+,\*</sup>*

#### *1. Particle Interactions*

We observe a small but significant increase in scattering intensity at low  $q$ -values when we reproduce the pH 7 data in Figure 1 with a sample containing additional small amounts of NaCl (ionic strength of solutions between 5 and 10 mM; see Fig. S1). At low ionic strengths we observe the influence of repulsive interactions between the proteins, a typical sign of which is the suppression of the scattering at low angles (low values of  $q$ ). It is therefore not correct to determine  $R_G$  from the sample at pH 7 without added salt as the Guinier extrapolation is valid for non-interacting particles only. However, samples with 5 and 7.5 mM NaCl respectively give very similar scattering curves with a flat plateau at small angles. This result suggests that at these salt and protein concentrations the proteins can be viewed as non-interacting. Increasing the NaCl concentration to 10 mM leads to an upturn of the scattering intensities at small angles, indicating that the interaction potential already became effectively attractive (Fig. S1). Therefore, the sample with 5 mM NaCl was used for the evaluation. At pH values lower than 7 only a very little influence of the salt concentration on the scattering curve is observed (Fig. S2). The intrinsic ionic strength at these pH conditions is sufficient to screen the electrostatic repulsions.

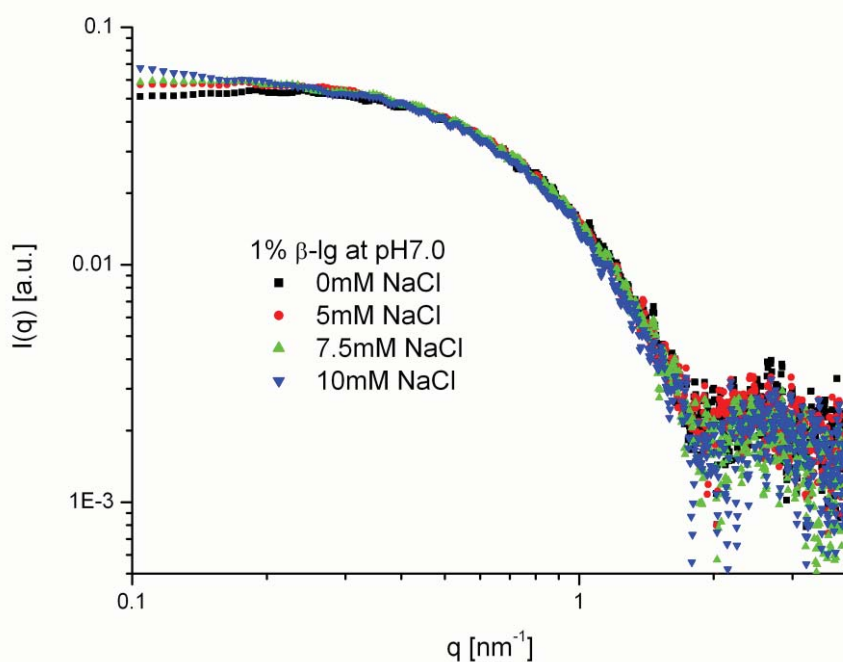


**Figure S1:** Subtracted small angle x-ray scattering curves (sample – water) of native 1 wt%  $\beta$ -Lactoglobulin solution at pH 7 and 25°C with different concentrations of added salt (data are slit smeared).

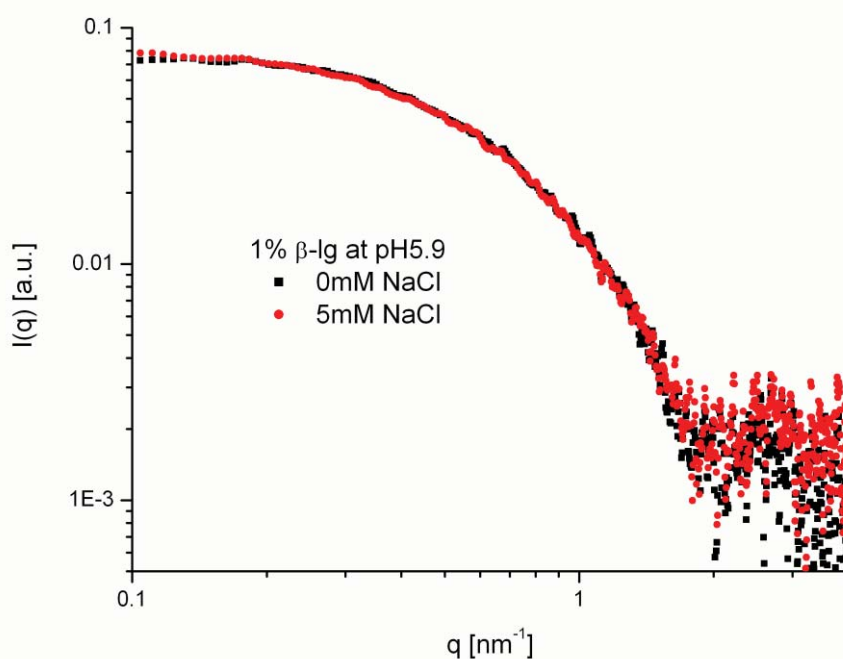


**Figure S2:** Small angle x-ray scattering curves (sample – water) of native 1 wt%  $\beta$ -Lactoglobulin solution at pH 5.9 and 25°C in water and with 5 mM NaCl added (data are slit smeared).

## 2. Stability of native protein solution

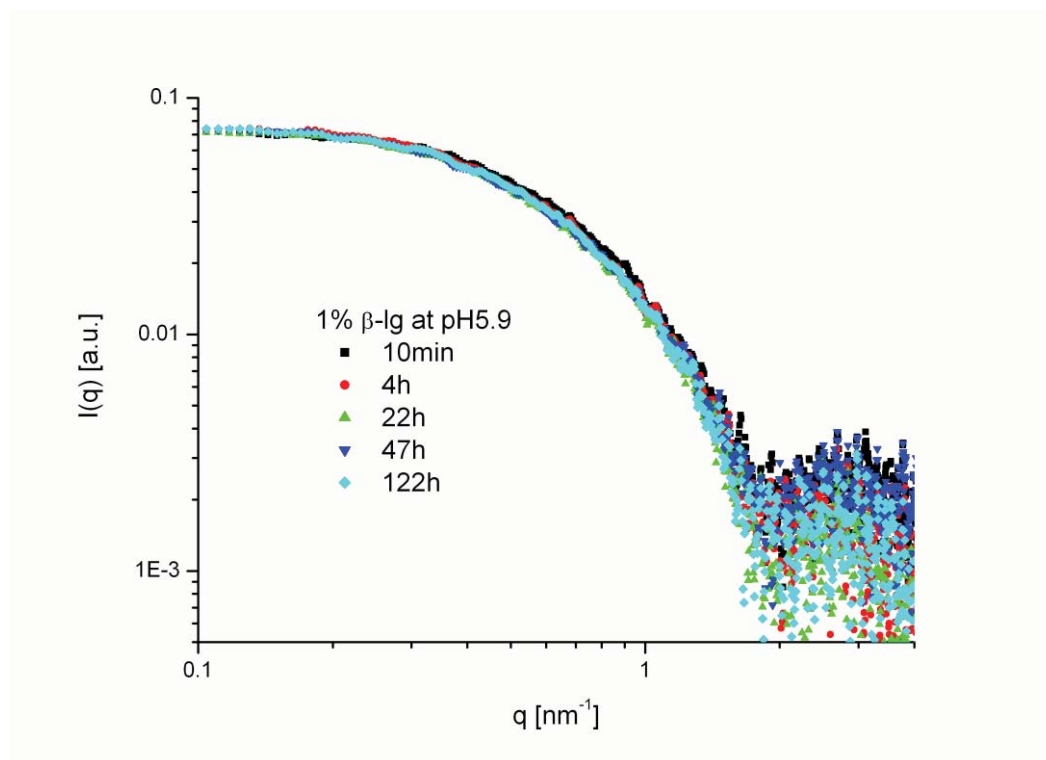


**Figure S3:** Small angle x-ray scattering curves of native 1 wt%  $\beta$ -lactoglobulin solution at pH 5.9 as a function of storage time at 25°C. No measurable changes can be found within the observation time (5 days).

## 3. Polydispersity of $M\beta$ lg – centrifugation experiment

In order to characterize the internal structure of  $M\beta$ lg the polydisperse sample was fractionated by mild centrifugation. After 6 hours of centrifugation at 450 g, a relatively narrow monomodal distribution was obtained. This can be seen from the extended linear range of the Guinier plot (Figure S4) and the weak angular dependence of the hydrodynamic radius (Figure S5). This sample now contains only one particular size distribution of  $M\beta$ lg and can thus be used to study the internal structure avoiding the difficulties connected with polydisperse samples. The ratio of  $R_G$  and  $R_H$  (extrapolation to a scattering angle of zero) is 0.6 and thus much smaller than 0.775, which is typical for homogeneous spheres. From Cryo-TEM it is known that  $M\beta$ lg are spherical in shape. Therefore we can conclude that the internal structure has to be inhomogeneous with a relatively dense core and a loose shell that contains more solvent.

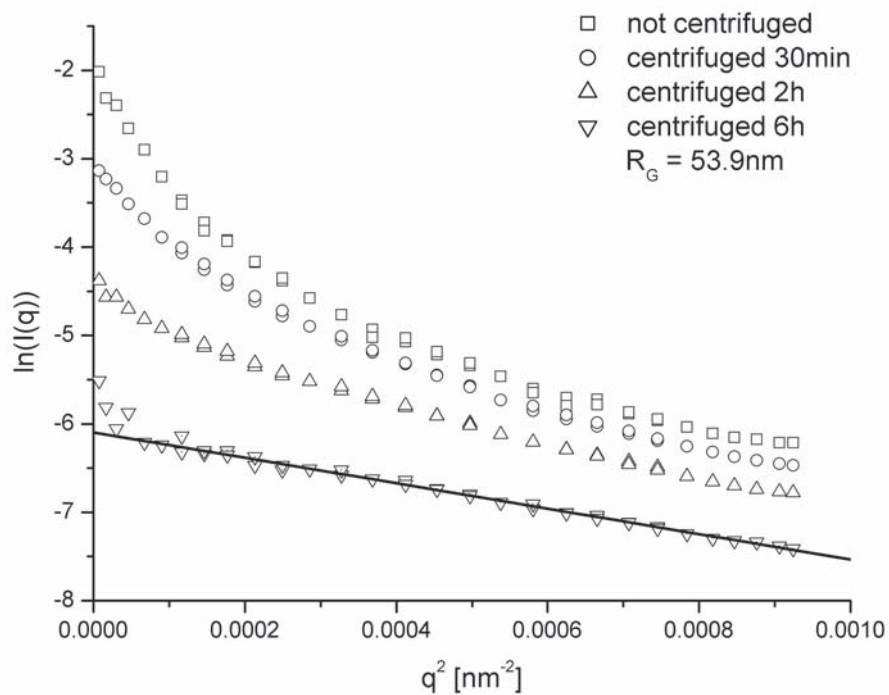


**Figure S4:** Guinier plot of static light scattering on  $\beta$ lg heated at 85°C for 15 min and after gentle centrifugation (450 g) for different times. A Guinier extrapolation could be performed after centrifugation for 6 h.  $R_G$  was 54 nm then while  $R_H$  (from DLS) of the same was 90 nm. Homogeneous spheres are characterized by a value for  $R_G/R_H = 0.775$ . Here we now measured  $R_G/R_H = 0.6$ , which is characteristic for particles possessing a rather dense core surrounded by a rather loose shell.

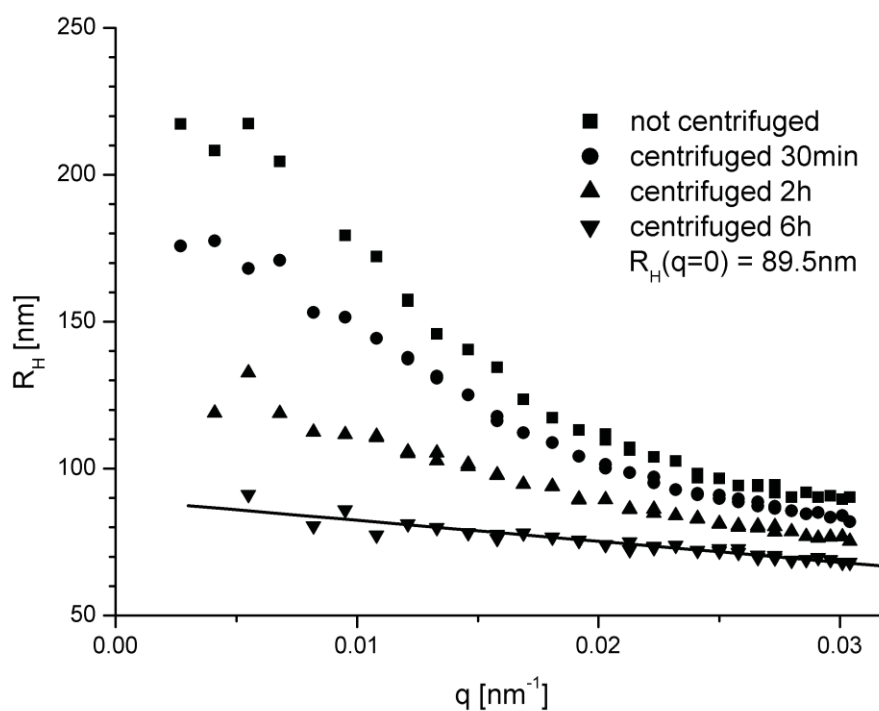


**Figure S5:** In agreement with the static intensities shown in Figure S6 also the dependence of the hydrodynamic radius is strongly affected by the polydispersity of the original sample. The larger particles contribute much more to the overall signal at small angles compared to large ones. In the observed angular regime ( $20 - 150^\circ$ ) the detected hydrodynamic radius drops from more than 200 to less than 100nm. After centrifugation for 6 hours only the smallest particles are left in the supernatant and the polydispersity is very much reduced. The decay in hydrodynamic radius with  $q$  is only very small and appears to be linear. This allows for an extrapolation to a scattering vector of zero.

#### 4. Polydispersity of M $\beta$ lg – angular dependence of hydrodynamic radius and polydispersity parameter.

Light scattering is very sensitive to impurities of large particles. Especially at small scattering angles they dominate the signal. Therefore, the angular dependence of the two parameters of the Cumulant analysis (hydrodynamic radius and polydispersity parameter) contains valuable information about the sample polydispersity. In Tables S1 and S2 the values obtained for various samples are summarized. The strong increase of  $R_H$  at small angles is an indication for the presence of large aggregates. If these large particles were absent,  $R_H$  would increase less steeply. For a perfectly monodisperse sample,  $R_H$  is constant and no angular dependence is expected.

**Table S1:** Angular dependence of the hydrodynamic radii  $R_H$  for all samples investigated by dynamic light scattering. For the interpretation mainly the value measured at  $120^\circ$  was used. However, the angular dependence contains valuable information about the sample polydispersity. Only for a perfectly monodisperse sample the measured  $R_H$  is independent of the scattering angle. For polydisperse samples  $R_H$  decreases with increasing scattering angle. Very large  $R_H$  values at very small angles indicate traces of impurities consisting of larger species.

Angle ( $^\circ$ )	q ( $\text{nm}^{-1}$ )	Native			Insoluble fraction								Soluble fraction							
		pH	pH	pH	70 $^\circ$	75 $^\circ$	80 $^\circ$	85 $^\circ$	85 $^\circ$	85 $^\circ$	85 $^\circ$	70 $^\circ$	75 $^\circ$	80 $^\circ$	85 $^\circ$	85 $^\circ$	85 $^\circ$	85 $^\circ$		
		7.0	5.9	2.0	0min				15min	1h	8h	0min				15min	1h	8h		
$R_H$	$R_H$	$R_H$	$R_H$	$R_H$	$R_H$	$R_H$	$R_H$	$R_H$	$R_H$	$R_H$	$R_H$	$R_H$	$R_H$	$R_H$	$R_H$	$R_H$	$R_H$	$R_H$		
(nm)	(nm)	(nm)	(nm)	(nm)	(nm)	(nm)	(nm)	(nm)	(nm)	(nm)	(nm)	(nm)	(nm)	(nm)	(nm)	(nm)	(nm)	(nm)	(nm)	
30	0.0082	7.4	548	56.8	315	257	210	225	218	238	251	190	111	82	96	83	50	40		
35	0.0095	6.9	476	42.4	305	254	197	191	201	201	215	176	101	70	79	78	47	37		
40	0.0108	5.3	438	16.6	294	219	188	175	193	190	195	158	98	63	80	75	45	37		
45	0.0121	3.5	387	7.0	296	196	166	165	185	178	189	141	92	62	76	73	46	34		
50	0.0133	2.5	358	11.5	280	184	156	159	164	175	183	128	90	57	73	70	42	33		
55	0.0146	2.8	236	5.9	255	168	150	151	160	169	175	120	87	54	68	71	42	32		
60	0.0158	3.4	183	3.2	249	158	144	146	158	163	169	106	85	55	71	70	42	31		
65	0.0169	2.5	108	2.8	242	151	140	145	152	160	173	99	81	48	65	66	39	31		
70	0.0181	4.3	90.0	2.4	230	142	139	142	150	156	162	93	77	49	63	64	39	31		
75	0.0192	3.9	75.1	4.6	225	139	136	137	146	152	164	85	76	46	63	61	36	30		
80	0.0203	2.2	31.3	3.9	219	135	133	139	146	150	156	80	75	43	59	57	37	29		
85	0.0213	3.5	23.2	2.5	197	129	130	133	151	144	160	74	73	42	55	58	35	28		
90	0.0223	2.7	18.7	3.8	186	126	129	133	147	144	152	71	72	42	54	53	34	27		
95	0.0232	1.8	11.4	3.9	196	125	128	128	143	146	155	67	70	38	53	52	33	28		
100	0.0241	3.7	9.3	3.9	179	122	126	128	142	140	153	62	67	38	50	49	32	28		
105	0.0250	4.2	8.5	3.3	175	119	125	128	141	144	153	59	66	36	49	47	31	27		
110	0.0258	3.3	7.7	3.6	181	118	121	127	142	140	151	57	65	34	47	44	30	27		
115	0.0266	2.8	8.0	3.1	172	117	122	126	149	138	149	54	63	32	45	45	30	26		
120	0.0273	3.2	6.5	3.7	156	113	120	126	138	141	150	55	61	31	42	44	29	26		
125	0.0280	3.0	6.5	3.4	165	110	119	124	142	140	148	53	60	29	41	42	28	26		
130	0.0286	3.4	6.6	3.3	159	110	118	123	141	139	147	50	59	28	40	40	28	25		
135	0.0291	3.2	6.5	3.3	165	110	118	123	139	143	149	49	59	28	39	37	28	25		
140	0.0296	3.1	6.1	4.1	157	108	117	123	143	139	151	46	57	27	37	36	27	25		
145	0.0301	3.0	5.9	3.3	148	107	115	123	135	139	151	46	57	27	37	35	26	25		
150	0.0304	1.8	6.2	3.7	166	107	114	122	138	142	146	45	56	27	36	35	26	25		

**Table S2:** Angular dependence of the polydispersity parameter of the cumulant analysis (PDI) for all samples investigated by dynamic light scattering. It is evident that the PDI of Mblg decreases during heating. Finally, a polydispersity of approximately 20% is achieved.

Angle (°)	q (nm <sup>-1</sup> )	Native			Insoluble fraction								Soluble fraction							
		pH 7.0	pH 5.9	pH 2.0	70°	75°	80°	85°	85°	85°	85°	70°	75°	80°	85°	85°	85°	85°		
		PDI (%)	PDI (%)	PDI (%)	PDI (%)	PDI (%)	PDI (%)	PDI (%)	PDI (%)	PDI (%)	PDI (%)	PDI (%)	PDI (%)	PDI (%)	PDI (%)	PDI (%)	PDI (%)	PDI (%)		
30	0.0082	44	46	48	19	30	17	14	24	26	17	36	29	41	38	46	42	40		
35	0.0095	50	48	47	27	26	29	25	23	25	18	34	30	41	34	45	41	41		
40	0.0108	46	47	44	22	30	18	17	17	13	20	34	28	42	34	47	42	40		
45	0.0121	41	48	43	32	29	20	22	22	22	19	36	29	43	36	47	41	39		
50	0.0133	46	48	42	30	29	23	19	19	14	20	37	28	43	38	48	42	39		
55	0.0146	45	47	45	28	28	19	18	15	20	21	37	29	41	38	48	42	37		
60	0.0158	45	46	49	32	30	20	20	19	17	16	39	29	43	37	48	42	38		
65	0.0169	54	45	49	35	26	17	12	17	17	17	38	30	45	39	47	40	38		
70	0.0181	45	44	48	32	26	15	20	22	16	22	38	32	43	39	47	40	38		
75	0.0192	47	44	37	35	25	19	12	21	19	17	40	32	45	38	46	41	37		
80	0.0203	53	43	41	35	27	20	17	20	17	19	40	31	45	40	45	41	37		
85	0.0213	50	44	52	36	28	20	21	20	16	18	41	32	45	42	44	42	37		
90	0.0223	49	44	39	34	25	23	16	16	20	17	41	31	47	41	45	41	37		
95	0.0232	51	44	36	37	26	18	19	19	21	24	41	33	46	42	44	42	37		
100	0.0241	42	43	32	36	28	20	16	20	22	19	42	35	44	40	43	41	37		
105	0.0250	42	43	42	36	28	21	17	15	20	19	43	35	45	42	44	42	37		
110	0.0258	42	43	32	38	26	21	19	20	22	18	43	35	45	43	44	42	36		
115	0.0266	41	43	40	38	25	24	24	22	21	24	44	35	46	43	43	42	36		
120	0.0273	41	43	36	37	27	20	19	21	20	19	42	35	46	44	44	42	35		
125	0.0280	40	43	35	35	26	15	20	20	18	18	44	36	45	41	44	41	38		
130	0.0286	43	43	27	33	27	19	20	21	19	19	43	35	45	42	43	42	37		
135	0.0291	41	42	35	39	26	22	22	23	20	21	43	37	46	45	42	41	36		
140	0.0296	41	41	31	39	27	24	24	20	24	22	44	38	47	45	43	42	35		
145	0.0301	41	39	30	38	29	22	24	26	24	24	44	37	46	44	36	41	36		
150	0.0304	45	39	27	41	28	26	24	25	23	22	45	35	45	44	42	42	36		